ference between **1** and **2** is of course due to the fact that singlet **2** succeeds in stabilizing itself in a manner not available to the tropyl radical, i.e., by valence tautomerism to cycloheptatetraene (**9**).

A preliminary search of the triplet potential surface showed that the conversion of **1** to **2** does not take place via triplet **10**. The transition state was not located precisely but its heat of formation was found to be close to, and not less than, 120 kcal/mol, corresponding to an activation energy of 18.5 kcal/mol and a reverse (**2** → **1**) activation energy of 26.5 kcal/mol. Such reactions would again take place very rapidly at 600 °C.

As noted above, **2**, when generated directly from the sodium salt of tropone tosylhydrazone (**5**), apparently fails[3e] to give the ring-contracted isomers **3** and **4** under conditions where these are formed[3c] by similar pyrolysis of the sodium salt of benzaldehyde tosylhydrazone (**12**). Crow and Paddon-Row[3c]

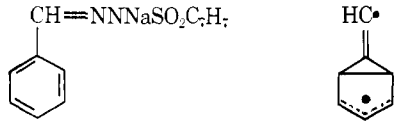

12 **13**

suggested that this difference might be due to the reactions taking place on surfaces of different multiplicity. If, as has been suggested,[3b] the conversion of **1** to **4** and **5** occurs via the biradical intermediate **13**, it is easily seen that this process could be very much easier on the singlet manifold because the difference in energy between the singlet and triplet forms of **14** must be quite small whereas that between singlet and triplet **1** is very large (33 kcal/mol according to MINDO/3). This explanation, however, depends on the assumption that while pyrolysis of **12** gives singlet **1**, pyrolysis of **5** gives triplet **2**. One would also have to assume that intersystem crossing between the singlet and triplet surfaces is slow on the time scale of a flash vacuum pyrolysis. These postulates seem rather difficult to justify.

Further work is clearly needed to clarify the reactions taking place in this very interesting system and such studies are in progress.

Acknowledgment. This work was supported by the Air Force Office of Scientific Research (Grant No. AFOSR-75-2749) and the Robert A. Welch Foundation (Grant No.F-126). The calculations were carried out using the CDC 6400-6600 computer at The University of Texas Computation Center. One of us (D.L.) acknowledges the award of a Robert A. Welch Postdoctoral Fellowship.

References and Notes

(1) Part 42: M. J. S. Dewar and H. S. Rzepa, *J. Mol. Struct.*, submitted.
(2) For general references, see M. J. Jones, Jr., *Acc. Chem. Res.*, **7**, 415 (1974).
(3) (a) W. J. Baron, M. Jones, and P. P. Gaspar, *J. Am. Chem. Soc.*, **92**, 4739 (1970); (b) E. Hedaya and M. E. Kent, *ibid.*, **93**, 3283 (1971); (c) W. D. Crow and M. N. Paddon-Row, *ibid.*, **94**, 4746 (1972); (d) P. O. Schissel, M. E. Kent, D. J. McAdoo, and E. Hedaya, *ibid.*, **92**, 2147 (1970); (e) C. Wentrup and K. Wilezek, *Helv. Chim. Acta*, **53**, 1459 (1970).
(4) R. Gleiter and R. Hoffmann, *J. Am. Chem. Soc.*, **90**, 5457 (1968).
(5) C. Cone, M. J. S. Dewar, and D. Landman, *J. Am. Chem. Soc.*, **99**, 372 (1977).
(6) R. C. Bingham, M. J. S. Dewar, and D. H. Lo, *J. Am. Chem. Soc.*, **97**, 1285, 1294, 1302, 1307 (1975).
(7) M. J. S. Dewar, R. C. Haddon, W. K. li, W. Thiel, and P. K. Weiner, *J. Am. Chem. Soc.*, **97**, 4540 (1975).
(8) J. W. McIver and A. Komornicki, *J. Am. Chem. Soc.*, **94**, 2625 (1972); **95**, 4512 (1973).
(9) Using a program written by Dr. P. K. Weiner.
(10) J. A. Pople and R. K. Nesbet, *J. Chem. Phys.*, **22**, 571 (1954).
(11) M. J. S. Dewar, A. Komornicki, D. Landman, S. H. Suck, and P. K. Weiner, unpublished work.
(12) A. G. Maki and R. A. Toth, *J. Mol. Spectrosc.*, **17**, 136 (1965).
(13) E. Wasserman, A. M. Trozzolo, W. A. Yager, and R. W. Murray, *J. Chem. Phys.*, **40**, 2408 (1964).
(14) Gleiter and Hoffmann also calculated (EH) this angle to be 143°. They gave arguments for believing that the experimental[13] value may be too large.
(15) P. F. Zittel, G. B. Ellison, S. V. O. Neill, E. Herbst, W. C. Lineberger, and W. P. Reinhardt, *J. Am. Chem. Soc.*, **98**, 3731 (1976).

Xα Multiple Scattering Calculations on Copper Porphine[1a]

David A. Case[1b] and Martin Karplus*

Contribution from the Department of Chemistry, Harvard University, Cambridge, Massachusetts 02138. *Received January 21, 1977*

Abstract: Spin-restricted and -unrestricted Xα calculations on copper porphine are performed and the results are compared with other calculations (EH, PPP) and the available experimental information; the latter include the redox properties, electronic spectra of the neutral species, the anion, and the cation, and high-resolution crystal ESR data. The relation of Xα eigenvalues to Hartree–Fock orbital energies is discussed. The ground state is formally Cu^{2+} (d^9), but formation of a d^{10} complex by reduction or charge-transfer excitation is predicted to occur at low energy. Some experimental evidence supports this prediction, although it is in disagreement with other calculations. Comparison of the charge distributions obtained by different calculations shows general agreement though there are some important differences. The effect of spin polarization on the orbital energies and coefficients is found to be small but not negligible. Perturbation theory is used to investigate the ESR spectrum. The calculated g values and hyperfine tensors are found to be in good agreement with experiment; an exception is the Fermi contact coupling, whose calculated value is too small by 35%. The ligand field description of ESR data is analyzed and it is shown that for copper porphyrin the conventional treatment yields qualitatively correct results but has quantitative deficiencies; the latter include neglect of charge-transfer excited states and the assumption of a single radial function for all copper 3d orbitals.

(I) Introduction

Metalloporphyrins have been prepared with most of the atoms of the first transition series.[2a] They have been intensively studied, both for their intrinsic interest and because of their biological importance. For the copper porphyrins, which correspond to a (Cu^{2+}, d^9) configuration, detailed high-resolution electron-spin resonance spectra are available.[2b] Additional data are provided by studies of the optical[3] and photoelectron spectra.[4] The interpretation of these results is simplified by the

fact that copper forms square-planar complexes, so that copper porphine (CuP) and the various porphyrins can to a good approximation be treated as systems with the full symmetry of the D_{4h} point group. The copper porphyrins, thus, are a set of compounds ideally suited for theoretical investigation. It is the object of the present paper to apply the Xα multiple scattering approximation[5-7] to copper porphine. The purpose of the study is threefold; first, to test the adequacy of the Xα method for large planar systems of this type; second, to obtain a more detailed interpretation of the available data; and third, to provide an essentially ab initio treatment on which simpler semiempirical models for such organometallic systems can be based.

At present, our knowledge of the quantitative molecular orbital structure of organometallic compounds is limited. Although a few ab initio studies exist, most of the work has been done with semiempirical models. The principal difficulty with the models has been to obtain parameters that are valid simultaneously for both first- and third-row atoms, especially since the latter may occur with a variety of formal charges. It is our hope that the Xα method, which was developed from the beginning with transition metals in mind, can help to clarify the situation. Of particular importance for the hyperfine interactions is the possibility of including spin polarization in a straightforward manner.

Section II outlines the method of calculation and contrasts certain of its attributes with the semiempirical approaches (extended Hückel, extended PPP) that have been used to study metalloporphyrins. In section III we examine the redox properties of the copper complexes with the goal of describing the nature of the orbitals involved. The Xα method seems particularly well-suited for this type of problem because of its independence of basis set limitations and the availability of "transition state" procedures to partially account for electronic relaxation effects. The relevant experiments include not only spectroscopic studies of the cation and anion, but also of the excited states of the neutral species resulting from charge transfer between the metal and the ligand. We shall see that in several instances the results of the present calculation are in better agreement with experiment than previous work.

The most detailed experimental comparisons involve the interpretation of ESR parameters, considered in section IV. The essentially ab initio Xα results are in excellent agreement with experiment. The use of a spin-unrestricted (UHF) formalism generally supports the standard molecular orbital scheme, although quantitative comparisons show significant deviations and suggest that caution is necessary in its application, particularly to systems with several unpaired electrons.

In spite of numerous applications of the Xα multiple scattering model to inorganic complexes,[6,7] the only reported applications to organometallic compounds have been to ferrocene[8] and Zeise's anion,[9] where a detailed test of the results is limited by the lack of data. The present study demonstrates that the characteristic interactions between metal d orbitals and ligand π orbitals can be represented successfully by an Xα calculation. Analogous applications to related systems, such as the iron porphyrins of biological importance, will be presented in subsequent publications.

(II) Method

In this section we briefly summarize the Xα method with emphasis on the points that are important for the present calculation. The difference in physical significance between certain of the Xα parameters and those of ordinary molecular orbital procedures is indicated.

(A) The Xα Multiple Scattering Method. The Xα scattered wave method has been the subject of a number of recent reviews.[5-7] The molecular spin-orbitals obtained in an Xα calculation are solutions of the one-electron differential equation (in atomic units) written for a spin ($+\frac{1}{2}$) electron (↑)

$$[-\tfrac{1}{2}\nabla_1^2 + V_c(1) + V_{X\alpha\uparrow}(1)]u_{i\uparrow}(1) = \epsilon(X\alpha)_{i\uparrow}u_{i\uparrow}(1) \quad (1)$$

where V_c is the classic Coulomb potential (nuclear attraction plus electron repulsion) and $V_{X\alpha\uparrow}$ is the local statistical exchange interaction between the electron in spin-orbital $u_{i\uparrow}$ and the other electrons; it approximates the nonlocal exchange term of the Hartree-Fock equation. The dependence of $V_{X\alpha\uparrow}$ on the charge density of spin-up electrons is

$$V_{X\alpha\uparrow} = -3\alpha\left(\frac{3}{4\pi}\rho_\uparrow\right)^{1/3} \quad (2)$$

with α an adjustable parameter taken from atomic calculations (see below). A spin-restricted calculation makes the assumption that the spin-up and spin-down densities are the same. Since both the Coulomb and statistical exchange potentials depend upon the charge density, the set of eq 1 must be solved iteratively to self-consistency as in a conventional Hartree-Fock calculation.

In the muffin-tin approach, eq 1 are solved approximately by replacing the potentials with their spherical averages inside spheres surrounding each nucleus. The radial Schroedinger equation is numerically integrated inside each sphere and the solutions matched at the boundaries to solutions in the intersphere region, where a constant potential is assumed. The boundary conditions at infinity are met by surrounding the entire molecule with an "outer sphere" and its spherically averaged potential, integrating inward from large distances, and again matching wave functions at the boundary. The matching conditions are expressed as an energy-dependent secular determinant, whose form has been given in detail by Johnson.[6] The resulting solution can be viewed as a special case of multipole analysis in a cellular method, as described by Williams.[10]

Once the molecular orbitals $u_{i\uparrow}, u_{i\downarrow}$ have been determined, expectation values of one-electron operators can be obtained by a method developed recently.[11] In this approach, the intersphere charge is apportioned among the atoms and represented by extending the radial wave functions a short distance beyond the atomic spheres. The overlaps of these orbitals are ignored, so that the calculation corresponds to that of the zero differential overlap approximation, with the exception that the "atomic orbitals" do not extend to infinity but only part-way to the nearest neighbor. This renormalization means that some care has to be used in comparing parameters, such as $\langle r^{-3}\rangle_{3d}$, which appears in the semiempirical evaluation of the hyperfine tensor. Due to renormalization, they will usually have a larger value in the scattered-wave model than in calculations employing a basis set of atomic orbitals, though the situation is more complicated if neighboring atom contributions are included; this point is considered in section IV with reference to the interpretation of ESR data.

The one-electron eigenvalues of eq 1 differ from their Hartree-Fock counterparts by not obeying Koopman's theorem. They are derivatives of the total energy with respect to occupation number,[5] that is,

$$\epsilon(X\alpha)_i = \partial\langle E_{X\alpha}\rangle/\partial n_i \quad (3)$$

If the total energy is approximated by a quadratic function of the orbital occupation number, the ionization potential of electron i may be calculated as the one-electron eigenvalue in a "transition state" model with half an electron in the orbital. We have

$$I_i \equiv \langle E_{X\alpha}(n_i = 0)\rangle - \langle E_{X\alpha}(n_i = 1)\rangle \simeq -\epsilon(X\alpha)_i(n_i = \tfrac{1}{2}) \quad (4)$$

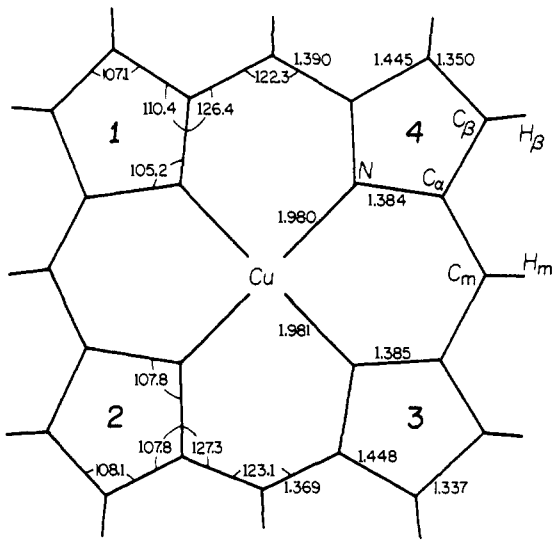

Figure 1. Geometry of copper porphine. Bond lengths in ångstroms and bond angles in degrees are shown for the assumed geometry (upper half of figure) and for crystals of α,β,γ,δ-tetraphenylporphinecopper(II) (lower half). The experimental results are from ref 16; values given are averages of lengths and angles that are equivalent in D_{4h} symmetry.

Since such a calculation includes to some extent the relaxation of the core upon loss of the electron, the method has proved quite successful in the interpretation of the photoelectron spectra of a wide range of compounds.[5-7] Electronic excitations can be treated in a similar manner by using a transition state with one-half electron in each of the spin orbitals involved in the transition. In this way, the state energy can be approximated by the one-electron eigenvalue difference.[5] The resulting value for the excitation energy accounts for two contributions not included in the Hartree-Fock orbital energy difference. The first of these is due to the change in Coulomb and exchange interactions on excitation. If these are obtained from the occupied and virtual orbitals of the ground state, they correspond to the second derivatives of the total Xα energy with respect to occupation number, calculated without allowing the orbitals to change.[5,12] The second effect is due to orbital relaxation, which generally reduces the unrelaxed corrections.[5] Both of these contributions are automatically included in the transition state procedure.

The above considerations must be kept in mind when comparing Xα eigenvalues with orbital energies from other one-electron theories. In particular, the Xα eigenvalues for the neutral molecule are always smaller in absolute magnitude than the corresponding ionization potentials. By contrast, the Hartree-Fock orbital energies are larger in magnitude than the ionization potentials, with the most important corrections to Koopman's theorem leading to smaller values.[13] Hence we expect the Xα and Hartree-Fock one-electron eigenvalues to bracket the experimental ionization potentials with the Xα values less negative than their Hartree-Fock counterparts. In spite of these differences, the two sets of level orderings and relative spacings can be quite similar. An analogous relation holds for the virtual orbital eigenvalues and molecular electron affinities. Again we expect the Xα and Hartree-Fock results to bracket the experimental number, with the Xα value this time more negative and the Hartree-Fock value more positive than the corresponding electron affinity.

For delocalized π orbitals, the corrections estimated from the difference between $\epsilon(X\alpha)_i(n_i = 1)$ and $\epsilon(X\alpha)_i(n_i = \frac{1}{2})$ are usually less than 0.1 eV. Thus, ionization potentials and transition energies can be estimated from the ground-state orbital diagram alone. For processes involving localized copper orbitals, however, it is essential to include the relaxation effects (see section IIIB).

Table I. Coordinates of the Unique Atoms[a]

Atom	x	y
Cu	0.0	0.0
N	0.0	3.741
C_α	2.077	5.331
C_β	1.276	7.941
C_m	4.601	4.601
H_β	2.492	9.581
H_m	6.045	6.045

[a] All atoms are in the *xy* plane; values are in au.

(B) Details of the Calculation. The results presented below were obtained with programs prepared by Johnson and Smith and kindly made available to us by Professor Johnson; for the one-electron property calculation an additional program described recently[11] was employed. Each iteration of the spin-restricted calculation required about 2 min of CPU time on an IBM 370/168. About 25 iterations were needed to converge the potential to a relative accuracy of 5×10^{-3} and the one-electron eigenvalues to an accuracy of 0.01 eV. Subsequent calculations for spin-unrestricted wave functions or for transition states generally converged more rapidly (in 5-10 iterations).

The geometry used has D_{4h} symmetry, corresponding to the unsubstituted copper porphine. The explicit effect of substituents was not included but is expected to be relatively small for most of the properties considered. The geometry closely mimics the crystal structure of bis(piperidine)-tetraphenylporphinatoiron(II), whose crystals exhibit only very small deviations from planarity in the porphine core.[14] The metal-nitrogen distance in this compound is 2.01 Å, typical of iron complexes.[15] To obtain a metal-nitrogen distance of 1.98 Å, equal to that found in copper tetraphenylporphine,[16] the four pyrrole groups were rigidly displaced toward the center of the system by 0.03 Å. Coordinates of the unique atoms are given in Table I, and Figure 1 compares the bond lengths and angles used with the average values found in crystals of copper tetraphenylporphine.

Values of α, the parameter in eq 2, were taken from atomic calculations:[17,18] Cu = 0.706 97, C = 0.753 31, N = 0.751 97, and H = 0.777 25. The α value for the inter-sphere and outersphere regions was set equal to that of carbon, which represents an intermediate value for the atoms of the molecule.

The partial wave expansions were truncated at $l = 4$ for the outer sphere, $l = 2$ for the copper sphere, $l = 1$ for those of carbon and nitrogen, and $l = 0$ for that of hydrogen. Hence the angular flexibility corresponds to a minimum basis set, though the radial flexibility, due to the numerical integration procedure used, is considerably greater. The radii of the regions around each nucleus were chosen so that the spheres overlap. This modification to the muffin-tin method was first introduced to provide a better description of organic molecules such as ethylene and benzene.[19] The nature of the approximations involved has been discussed by Herman, Williams, and Johnson,[20] and a number of studies of the effect of changing sphere radii have appeared.[21-23] Of particular interest is the work of Herman and co-workers on the TCNQ molecule,[20,21] which like porphine is a large planar π-bonded organic molecule. Herman et al. tried a number of different sets of sphere radii and found one (model IV) that gave the best agreement with experiment. Since the porphine ring system is nearly twice as large as TCNQ, it is expensive to go through a corresponding study of the variation of sphere radii. The radii used in the present calculation were chosen as follows: the values for carbon and nitrogen (both $1.60a_0$) and for hydrogen ($0.95a_0$) were taken from calculations on the single-ring heterocycles pyridine and pyrrole, which will be discussed elsewhere.[24] The model IV values of Herman et al.[20] for TCNQ were C =

1.63a_0 (average), N = 1.50a_0, and H = 1.01a_0. The two sets of radii are thus very similar; the main difference is in the nitrogen, which in TCNQ is in a triple bonded cyano group and so would be expected to have a smaller orbital radius than the aromatic porphyrin nitrogens. Our value for the carbon sphere radius is also in good agreement with values used in previous studies on benzene,[19] formaldehyde,[22] and $Fe(SCH_3)^{4-}$.[25] Our hydrogen radius is 0.1 to 0.3a_0 smaller than those chosen in the earlier work, but we do not expect this to strongly affect the π bonds of most importance to this study; test calculations on smaller compounds have confirmed this conclusion.[24] The copper radius (2.62a_0) was that used for iron in previous calculations on ferrocene[8] and by the authors in concurrent studies of iron porphine. It is close to the value of 2.50a_0 chosen for iron by Norman[25] for the iron-sulfur center in rubredoxin. It would be useful to have a comparison of results obtained with a different radius for the copper since certain aspects of the calculation may be sensitive to its value. However, the expense of the porphyrin calculations suggests that such studies should be made on simpler model systems. The outer-sphere radius was 10.6a_0, which overlaps slightly with the spheres of the outermost hydrogens. The resulting virial ratio, $-V/T$, was 1.98 to 1.99 for these calculations; this has been used as a criterion for choosing radii by some authors[20] and the present value indicates that reasonable values have been selected.

Although no completely satisfactory nonempirical method for the selection of sphere radii exists,[25] the present choice appears to be satisfactory and serves to make our results comparable to other studies. It is unlikely that the results could be significantly altered by variations of the sphere radii within a reasonable range.

(III) Results and Discussion

In this section we consider first the copper porphine energy levels and the resulting spectroscopic and redox properties. We then present the details of the wave function and use it and the energy levels for an interpretation of the ESR spectrum. Both a standard treatment of the ESR parameters based on a single orbital perturbation scheme and a more general unrestricted wave function analysis are described.

(A) One-Electron Eigenvalues. Copper porphine is a neutral 189-electron system that formally consists of one Cu^{2+} ion (27 electrons) and one porphine ion (P^{2-}) (20 C, 4 N, 12 H with 162 electrons). In the Xα ground state there are 94 doubly occupied orbitals and one singly occupied orbital ($7b_{1g}$). Table II lists the outer valence shell orbitals in the spin-restricted and -unrestricted calculations, including the unoccupied orbitals that play a role in various of the properties discussed subsequently. In addition, a footnote to the table gives the energies of all the deeper valence shell and inner shell orbitals in the restricted calculation. The character of the important valence orbitals (i.e., the major contributions) is also indicated in the table.

Figure 2 compares the highest occupied and lowest unoccupied levels with the results of two previous calculations, one that used the iterative extended Hückel method,[26] and the other an extended Pariser-Parr-Pople or "peel electron" scheme.[27] The ordering of levels in the three calculations is very similar, both for the mainly metal and mainly porphine orbitals. The major differences occur for the relative positions of metal and ligand orbitals. Most important is the relation of the singly occupied ($7b_{1g}$) orbital, which is primarily copper $3d_{x^2-y^2}$, to the top filled $1a_{1u}$,$3a_{2u}$ pair of porphyrin π orbitals. In the extended Hückel calculation, the copper orbital is 1.5 eV above the ligand level; the PPP result has an even larger difference, the copper orbital being 4.0 eV higher; while the Xα calculation shows the $7b_{1g}$ orbital to be 1.35 eV *below* the porphyrin π pair ($1a_{1u}$,$3a_{2u}$). Although the Xα eigenvalues are

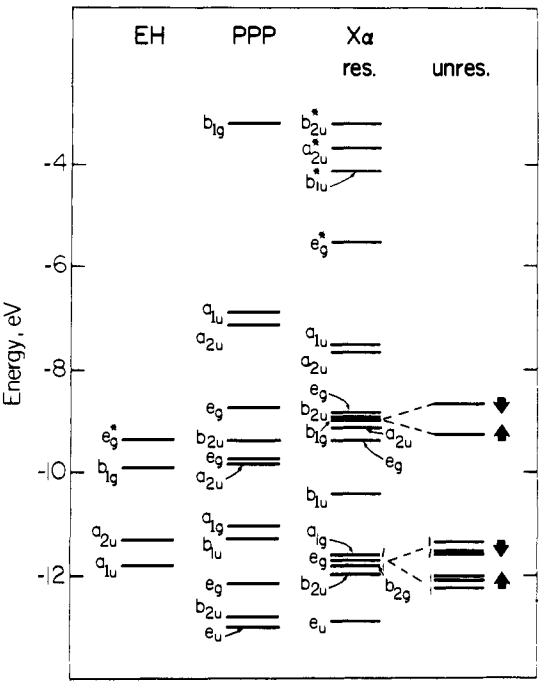

Figure 2. Orbital energies; extended Hückel results are from ref 26, extended Pariser-Parr-Pople results from ref 27.

not strictly comparable to Hartree-Fock energies (see section II), such large deviations, particularly with respect to the PPP calculations, are expected to lead to qualitatively different descriptions of the electronic structure. We discuss below experimental evidence favoring the Xα results.

It is worth noting that the relative stability of metal and ligand orbitals is a point on which semiempirical methods are especially dependent upon the parameterization. Zerner, Gouterman, and Kobayashi[28] give an example of a second "reasonable" set of ionization potentials for the extended Hückel theory in which the metal levels are shifted by nearly 1 eV from their standard positions. As to the Xα results, there may also be some sensitivity to changes in the relative sphere radii and the resulting amount of overlap.

The lower Xα virtual orbital energies in Table II are seen to be negative, in contrast to the usual behavior for Hartree-Fock energies of neutral systems. This difference reflects the fact that the effective one-electron potential is the same for all orbitals in the present calculation, while in the Hartree-Fock scheme the virtual orbitals see a neutral core representing all of the other electrons.

The spin-unrestricted results shown in Table II and Figure 2 are representative of a general pattern in organometallic compounds. The highly delocalized ligand π orbitals (e.g., $1a_{1u}$, $3a_{2u}$, $3e_g$) see little exchange effect and the splitting between spin-up and spin-down orbitals is very small. By contrast, the molecular orbitals that are mainly 3d and localized on the copper (e.g., $7b_{1g}$, $6b_{2g}$, $2e_g$) have a sizable splitting. Even for the spin $^1/_2$ system, the separations can be on the order of 0.5 eV. In addition to altering the positions of expected electronic transitions, shifts of this magnitude also change the amount of ligand mixing in the molecular orbitals. For metals such as iron, which can have up to five unpaired electrons, such exchange effects may have to be included (as they are in an unrestricted calculation) to arrive at even a qualitative understanding of the electronic structure.

Table III lists the most important orbital populations obtained from the Xα calculation and the previously published extended Hückel and PPP calculations. The general features of the populations are similar, though there are significant differences; e.g., the nitrogen π orbitals have a larger popula-

Table II. One-Electron Eigenfunctions and Eigenvalues[a]

Orbital	Energy, eV[b]	Description[c]
	−3.23	
$3b_{2u}$*	−3.20 −3.15	0.071 N + 0.076 C_α + 0.013 C_β
	−4.13	
$2b_{1u}$*	−4.13 −4.13	0.013 C_α + 0.067 C_β + 0.090 C_m
	−5.57	
$5e_g$*	−5.55 −5.54	0.030 N + 0.042 C_α + 0.031 C_β + 0.069 C_m
	−7.56	
$1a_{1u}$	−7.56 −7.55	0.099 C_α + 0.026 C_β
	−7.67	
$3a_{2u}$	−7.65 −7.62	0.027 Cu(p_z) + 0.050 N + 0.018 C_β + 0.141 C_m
	−8.93	
$4e_g$	−8.88 −8.81	0.041 Cu(dπ) + 0.091 N + 0.069 C_β
	−8.92	
$2b_{2u}$	−8.89 −8.85	0.085 N + 0.081 C_β
	−9.18	
$7b_{1g}$	−8.95 −8.69	0.617 Cu($d_{x^2-y^2}$) + 0.018 N (2s) + .057 N($2p_\sigma$)
	−9.18	
$2a_{2u}$	−9.15 −9.11	0.031 Cu(p_z) + 0.074 N + 0.083 C_β
	−9.40	
$3e_g$	−9.40 −9.39	0.056 C_α + 0.026 C_β + 0.077 C_m
	−10.46	
$1b_{1u}$	−10.46 −10.46	0.065 C_α + 0.108 C_m
	−12.06	
$8a_{1g}$	−11.64 −11.37	0.098 Cu(4s) + 0.851 Cu(d_{z^2})
	−12.09	
$2e_g$	−11.78 −11.56	0.703 Cu (dπ) + 0.017 C_α + 0.11 C_β + 0.011 C_m
	−12.26	
$6b_{2g}$	−11.80 −11.52	0.935 Cu(d_{xy})
	−12.05	
$1b_{2u}$	−12.01 −11.97	0.098 N + 0.047 C_α + 0.030 C_β

[a] Lower lying orbital energies (eV) for the spin-restricted calculation: core orbitals, Cu(1s), -(2s), -(3s) = −8747.3, −1047.22, −117.55; Cu(2p), -(3p) = −920.63, −78.06; N(1s) = −384.30; C_α(1s) = −274.73; C_β(1s) = −273.13; C_m(1s) = −273.68; valence orbitals, a_{1g} = −28.95, −24.56, −23.73, −18.13, −15.39, −15.51, −14.45; b_{1g} = −28.54, −24.38, −20.18, −17.25, −15.02, −14.09; a_{2g} = −22.75, −18.19, −16.41, −13.54; b_{2g} = −25.35, −19.14, −18.95, −14.57, −13.71; e_g = −12.93; a_{2u} = −12.98; e_u = −28.73, −24.80, −24.32, −21.50, −18.69, −17.82, −17.02, −15.17, −14.72, −13.65, −12.92. [b] The restricted value is given at the left, with the unrestricted values to the right, spin-up levels listed above spin-down levels. [c] Populations in the restricted theory for various atoms (Figure 1); orbitals shown are π orbitals, except for $7b_{1g}$, $8a_{1g}$, and $6b_{2g}$; populations for e_g orbitals are averages of the degenerate pair.

Table III. Electronic Populations

Atomic orbital	Xα[a]	PPP[b]	EHT[c]
Porphin π:			
N	1.511	1.470	1.378
C_α	0.988	0.977	1.058
C_β	0.989	1.022	1.006
C_m	0.973	1.017	0.958
Total	25.75	25.94	25.86
Copper:			
$3d_{z^2}$	2.006	1.955	2.0[d]
$3d_{xy}$	1.997	2.000	2.0[d]
$3d_{x^2-y^2}$	1.696	1.288	1.681[d]
$3d_{xz}$, d_{yz}	2.027	1.962	1.992
4s	0.713	0.548	0.488
$4p_x$, p_y	0.438	0.174	0.205
$4p_z$	0.140	0.135	0.157
Total	11.48	10.20	10.72
Net Cu	−0.482	+0.801	+0.281

[a] This work, unrestricted calculation. [b] From ref 27. [c] From ref 26. [d] Calculated from data in ref 23 assuming the d_{z^2} and d_{xy} orbitals to be completely filled.

tion in the Xα than in both the PPP and the EHT results and the ordering of the carbon charges varies among the three calculations. On the copper, the largest difference is between the PPP and the Xα or EHT results, with the $3d_{x^2-y^2}$ much less populated in the former than in the latter; this is probably a consequence of the limited σ-orbital basis in the extended PPP formalism. The Xα calculation also gives more weight to the 4s, $4p_x$, and $4p_y$ orbitals than do the other two. The resulting net copper charge is −0.5 in the Xα calculation, significantly different from the slightly positive values expected and found in the PPP (+0.8) and EHT calculations (+0.3). Which result is correct is not clear since there is no direct criterion for determining atomic charges. One type of correlation that has been used is that between the inner-shell energy levels and the net charge.[29] Table IV compares the calculated Xα values obtained for the copper porphine in both the restricted and unrestricted calculations with those obtained for an isolated Cu^+ ion ($3d^94s$) and a neutral Cu atom ($3d^94s^2$). As can be seen, the Cu porphine results are *intermediate* between the two and somewhat closer to neutral Cu. The calculated self-consistent potential shows corresponding behavior; in the inner region it is 1-2 eV below the atomic value and this difference increases in the overlap region due to the effect of the partially shielded nitrogen cores. These results indicate that the net charge, per se, is not too meaningful a quantity. In part this is due to the somewhat arbitrary procedure used in its evaluation. Additional information on the validity of the Xα charge distribution is given in section IIIC.

The Xα wave functions obtained here are the self-consistent solutions in a field corresponding to a closed-shell porphine and a d^9 copper ion. This is in agreement with the ESR and the spectral properties of the compound, as we see in sections IIIB and IIIC. We must now show that this choice of orbital occupations yields the ground state of the system. This is not immediately obvious since the only half-filled orbital ($7b_{1g}$) has a lower energy than the doubly filled $1a_{1u}$ and $3a_{2u}$ level (see Table II). No such question arises in the PPP or EHT calculation, in which the b_{1g} level is above a_{1u} and a_{2u}. The present situation is analogous to that in atomic copper, where the configuration $(3d)^9(4s)^2$ has the partially empty 3d↓ level below both the 4s↑, 4s↓ levels. In both the atomic and molecular cases the ground state may be determined by performing a transition state calculation; for the molecule, the transfer of ½ electron from the a_{1u} orbital to the b_{1g} orbital provides an estimate of the energy difference between the chosen ground-state configuration and that corresponding to a closed-shell (d^{10}) copper atom and a porphyrin π-cation radical. The results of such a calculation are given in Table V. It can be seen by comparing the $1a_{1u}$ and $7b_{1g}$ spin-down energies that the d^{10} state is predicted to be approximately 0.2 eV above the d^9 state. Corresponding behavior has been observed in ordinary Hartree-Fock calculations of transition metal complexes; a detailed discussion is given by Demuynck and Veillard with reference to $CuCl_4^{2-}$.[30]

The copper-nitrogen distance plays an important role in the state ordering. A separate calculation with a Cu-N distance of 2.01 Å results in the two states (Cu^{2+}, P^{2-}, and Cu^+, P^-) having nearly equal energy. This strong dependence on geometry is largely due to the repulsive effect of the occupied nitrogen orbitals on the energy of the Cu $3d_{x^2-y^2}$ orbital. Hence the ground state of copper porphine is predicted to change from $^2B_{1g}$ to $^2A_{1u}$ near a Cu-N distance of 2.01 Å. Similar state crossings have been seen in our calculations on iron porphyrins,

Table IV. Self-Consistent Potentials[a] and One-Electron Energies

				CuP(unres)	
r^b	Cu^+	Cu^0	CuP(res)	↑	↓
0.055	−432.18	−431.83	−431.90	−431.90	−431.90
0.138	−132.83	−132.49	−132.55	−132.55	−132.55
0.305	−40.11	−39.77	−39.83	−39.85	−39.82
0.640	−9.86	−9.51	−9.58	−9.61	−9.57
0.870	−5.00	−4.65	−4.73	−4.75	−4.72
1.308	−2.09	−1.73	−1.85	−1.86	−1.85
1.769	−1.18	−0.84	−1.01	−1.01	−1.01
2.645	−0.62	−0.33	−0.68	−0.69	−0.68
ϵ(1s)	−8754.1	−8745.9	−8747.3	−8747.3	−8747.3
ϵ(2s)	−1054.7	−1045.5	−1047.2	−1047.3	−1047.0
ϵ(3s)	−124.8	−115.4	−117.5	−118.0	−117.1
ϵ(2p)	−928.2	−918.9	−920.6	−920.8	−920.4
ϵ(3p)	−85.2	−75.9	−78.0	−78.5	−77.6

[a] Potentials in au; one-electron energies in eV. [b] Distance from copper nucleus in au.

where spin and stereochemical changes are known to be closely linked.

(B) Oxidation–Reduction and Electronic Spectrum. It is clear from Figure 2 that the metal d orbitals are lower in energy relative to the ligand π orbitals in the Xα calculation than they are in extended Hückel or PPP theory. This difference leads to the expectation of more facile reduction to Cu^+ and of lower-lying ligand-to-metal charge-transfer transitions in the Xα description of the copper porphyrins. The details of these predictions and other aspects of the electronic spectrum are discussed and compared with experiment in what follows.

Oxidation–Reduction. The interpretation of ionization potentials and photoelectron spectra has been one of the most common uses of Xα calculations. For most of the systems studied, satisfactory results have been obtained for the relative ordering and spacing of the ionized states. As with ab initio calculations, the absolute energy values are found to be less accurate than the relative energies. Indeed, the work of Herman et al.[20,21] on TCNQ was based in part on fitting the first calculated ionization potential to the experimental value. It was noticed that the size of the outer sphere had a marked effect on the absolute values of the energies but little effect on the energy differences of the upper orbitals. We have seen the same behavior in iron porphyrin calculations; that is, an increase in the outer sphere radius lowers all of the π levels by nearly the same amount. This is a consequence of the increase in size of the inter-sphere region and the volume averaging of the electronic charge, which leads to less shielding of the nuclei and a resulting stabilization of all of the energy levels. The effect is especially pronounced for planar molecules enclosed in spherical cavities, as are the various porphyrins. Although proposals have been made to overcome this problem by the introduction of nonspherical cavities, the standard approach was used in the present study.

The transition-state result for the first ionization potential of copper porphine is 9.1 eV, higher than the value of 7.1 eV estimated from liquid-phase polarographic measurements[31] and the value of 6.5 eV from the photoelectron spectrum of copper tetraphenylporphine (CuTPP).[32] A calculation on the constituent pyrrole[24] led to a predicted first ionization potential of 9.4 eV, which is larger than the observed value of 8.3 eV.[33] (The pyrrole calculation used the sphere radii given in section II and an outer sphere tangent to the molecule.) The lowering of the experimental ionization potential with the increase in size of the conjugated system is analogous to the results obtained for polyacenes;[34] e.g., the ionization potential of naphthacene is 2.4 eV below that of benzene. The Xα difference in ionization potential between Cu porphine and its constituent pyrroles is too small; this may reflect the uncertainties in choosing sphere radii, which are known to have a strong effect on ionization potentials.[20,24]

Table V. One-Electron Energies for $1a_{1u}\downarrow$ to $7b_{1g}\downarrow$ Transition State[a]

$1a_{1u}$	−7.58 −7.50	$3e_g$	−9.39 −9.34
$3a_{2u}$	−7.56 −7.53	$1b_{1u}$	−10.45 −10.41
$4e_g$	−8.67 −8.54	$8a_{1g}$	−10.12 −9.68
$7b_{1g}$	−7.74 −7.31	$2e_g$	−10.46 −10.07
$2b_{2u}$	−8.80 −8.75	$6b_{2g}$	−10.22 −9.74
$2a_{2u}$	−9.06 −9.01	$1b_{2u}$	−11.93 −11.85
		$1e_g$	−12.63 −12.56

[a] Spin-up levels are listed above the spin-down levels. The $1a_{1u}\downarrow$ and $7b_{1g}\downarrow$ levels have occupations of 0.5; all other levels listed are fully occupied.

The above discussion assumes that the ionized electron comes primarily from the porphine. This follows from Table II and Figure 2, which suggest that the porphine π-cation radical is a $^2A_{1u}$ state with the $^2A_{2u}$ state only 0.09 eV higher in energy. ESR and visible spectra can be used to characterize the porphyrin π-cation radicals formed from oxidation of metalloporphyrins. Dolphin and Felton[35] have identified certain patterns in the visible spectrum as characteristic of abstraction from either the $1a_{1u}$ or the $3a_{2u}$ orbital. Both copper tetraphenylporphine and copper octaethylporphine display spectra characteristic of oxidation from the latter orbital to create a $^2A_{2u}$ cation, which couples with the unpaired copper spin to form singlet and triplet states. Thus, experiment agrees with the Xα result that the first electron is removed from the porphine but disagrees as to the resulting state symmetry. Since the present calculations were performed without peripheral substitutents, they may be insufficiently precise to distinguish between $^2A_{1u}$ and $^2A_{2u}$ radicals. Application of Koopman's theorem to either the EHT or the PPP results would lead to the prediction of electron abstraction from the metal. Koopman's theorem is not valid for the open-shell eigenvalue in the PPP calculation, but it is not clear that a correct calculation of the ionization potential would change the order.

Also of interest are the reduction properties of the copper porphyrins. Here, the nature of the orbitals accepting the electron is less well-characterized. Felton and Linschitz[36] noticed that the reduction potentials for a series of metallo-

porphyrins were fairly independent of the metal and concluded that the first reduction takes place into the porphyrin e_g^* orbital. More direct x-ray photoelectron evidence in the solid state shows shifts in the Cu $^2P_{3/2}$ line, which is indicative of reduction of the copper.[4] Transition-state calculations for reduction at both the metal $7b_{1g}$ and the ligand $5e_g^*$ orbitals yield an energy of -5.6 eV for the former and -3.9 eV for the latter. The prediction of reduction at the metal is directly related to the low energy of the Cu d orbitals in the ground state. By contrast, the level ordering of the extended Hückel theory leads to the expectation that the additional electron will go into a porphyrin orbital.[4,26]

Electronic Spectrum. The strong visible and Soret bands of the copper porphyrins correspond to a "normal" porphyrin spectrum, consisting of transitions from the near-degenerate a_{1u},a_{2u} to the e_g^* levels.[37] The observed transitions are known to involve a large amount of configurational mixing so that an energy level diagram, such as Figure 2, cannot be correlated directly with the individual transitions even in the Xα formulation. However, the *average* energy of the transitions should be given by the calculation. Zerner and Gouterman estimated the experimental average energy for the singlet and triplet transitions from a_{1u},a_{2u} to e_g^* to be 2.19 eV, in very good agreement with the Xα value, which is 2.05 eV. It may be mentioned that in the EHT calculations the experimental value of 2.19 eV was used in adjusting the parameters of the model.[26] Transition state calculations should not be necessary here since all of the orbitals are extensively delocalized and located in roughly the same parts of space.

For evaluating the charge-transfer transitions, which involve highly localized metal d orbitals whose energy is quite sensitive to the charge on the copper atom, a transition state calculation is required. It is possible to use for this purpose the results obtained earlier in determining the ground state of the system (Table V); in this calculation half an electron was transferred from the a_{1u} orbital of the porphyrin to the $7b_{1g}$ orbital, which is mainly $3d_{x^2-y^2}$ on the copper atom. Using levels shown in Table V as a guide for the location of the ligand-to-metal transitions involving porphyrin π orbitals and the copper $3d_{x^2-y^2}$ state, we see that the lowest optically allowed transition is calculated to be $2b_{2u}$ to $7b_{1g}$ at about 1.49 eV; the importance of the transition state calculation is made clear by comparing this result with Table II, in which the $7b_{1g}$ level is actually *below* $2b_{2u}$. The energy of the $2b_{2u} \rightarrow 7b_{1g}$ transition is not far from the weak transition seen in CuTPP at 1.73 eV;[38,39] however, there is the alternative possibility that the transition involves "tripdoublet" states, corresponding to porphyrin triplet excitations[39] that are also expected to be weak and located in this region. It should be noted that there is a significant disagreement between the Xα results and the extended PPP calculations;[27] the latter show no ligand-to-metal transitions below 5 eV.

Table II indicates that the energy for the lowest charge-transfer transition from the metal to ligand orbitals is $\gtrsim$4.0 eV; this is based on the assumption that a transition-state calculation would lower the copper d levels by at least 1 eV, in accord with corresponding atomic transition state results.[5] Hence the observed weak transition at 4.1 eV[38] could involve a metal-to-ligand transfer. This contrasts with both the EHT calculations[26,40] which place the $7b_{1g}$ to $5e_g^*$ transition at 0.45 eV, and PPP calculations,[27] which give a value of 2.45 eV. Other comparisons have indicated that the EHT value is likely to be an underestimate,[40] but there is insufficient experience with PPP calculations of this type to make a judgment on the expected error.

The final type of transition is the class of forbidden d-d bands, which are not expected to be intense enough to be easily observed. The energy differences involved are important for the interpretation of spin-orbit effects and are discussed more fully in the section on ESR (see section IIIC). The Xα value of $\sim$2.8 eV for both $\Delta_\perp$ and $\Delta_\parallel$, defined by

$$\Delta_\perp = \epsilon(7b_{1g}) - \epsilon(2e_g)$$

$$\Delta_\parallel = \epsilon(7b_{1g}) - \epsilon(6b_{2g})$$

is in agreement with the accepted estimates of the splitting in the Cu porphyrins. By contrast, Guzy et al.[41] suggest that the transitions at 1.7 and 2.0 eV in copper phthalocyanine may be d-d bands. This is not consistent with the present results and the expectation that the crystal field splittings will be higher in the phthalocyanins than in the porphyrins because of the shorter Cu-N distance in the former. The Xα calculations yield no such bands below about 2.5 eV. The extended PPP calculations give $\Delta_\perp = 2.78$ eV and $\Delta_\parallel = 3.21$ eV.

(C) Electron Spin Resonance Results. A large number of experimental spectra have been recorded for copper porphyrins[26,42-44] and the analogous phthalocyanines.[45,46] Perhaps the most complete study is that of copper tetraphenylporphine by Manoharan and Rogers (MR);[44] they made measurements on magnetically dilute single crystals, as well as on solutions and polycrystalline powders. Hyperfine splittings were seen from both copper and the ligand nitrogen atoms. Later work has made use of isotopically pure ^{63}Cu to simplify the hyperfine spectrum. A review of the rather extensive literature on the ESR of Cu porphyrins has been presented by Lau and Lin.[2b] The ESR data will be interpreted in two ways. First, we shall calculate the expected spectrum in the most straightforward way by employing the "conventional state of the art perturbation approach".[47] However, rather than using the experimental data to determine the form of the wave function (as is usually done), we obtain the required covalency parameters and orbital energies from the Xα calculation. This permits a comparison between the "experimental" MO structure and that determined by theory. In the second part of this section, we examine some corrections to the conventional treatment and consider their effect on the usual interpretation of the ESR spectrum in terms of molecular parameters. The two types of approaches provide a detailed analysis of the ESR spectrum, including a somewhat altered meaning for some of the parameters in the simple molecular orbital picture.

Conventional Perturbation Treatment. The analysis of transition metal ESR is generally based on the perturbation method introduced by Abragam and Pryce[48] for the crystal field model and subsequently modified to include the effects of covalency.[49,50] The general subject is reviewed in the classic text by Abragam and Bleany[47] and the application of the theory to square-planar copper compounds is given in detail by Kuska and Rogers.[47] In what follows, we outline only the parts of the formulation necessary for the present analysis. It is assumed that a restricted molecular orbital wave function is being used as the unperturbed function with the unpaired spin entirely in the $7b_{1g}$ orbital. Orbital mixing occurs through the perturbation due to spin-orbit coupling.

The relevant molecular orbitals for D_{4h} symmetry can be expressed in the form (for orbital numbers, see Table II)

$$\begin{aligned} 7b_{1g} &= \alpha d_{x^2-y^2} - \tfrac{1}{2}\alpha'[-\sigma_1{}^x + \sigma_2{}^y + \sigma_3{}^x - \sigma_4{}^y] \\ 6b_{2g} &= \beta d_{xy} - \tfrac{1}{2}\beta'[p_1{}^y + p_2{}^x - p_3{}^y - p_4{}^x] \\ 2e_g &= \begin{bmatrix} \delta d_{xz} - \dfrac{\delta'}{2^{1/2}}[p_1{}^z - p_3{}^z] \\ \delta d_{yz} - \dfrac{\delta'}{2^{1/2}}[p_2{}^z - p_4{}^z] \end{bmatrix} \end{aligned} \tag{5}$$

These occupied orbitals are important because they have the largest contribution from the copper atom and hence are expected to mix most strongly with the ground state by spin-orbit coupling; the corrections due to other molecular orbitals are

considered subsequently. The symbols σ and p represent the nitrogen ligand functions of the indicated symmetry; the numbers label the nitrogen atoms as in Figure 1. The σ functions are the appropriate hybrids of the ligand nitrogen 2s and 2p orbitals. The molecular orbital coefficients α, β, δ can be obtained from the spin-restricted ground-state wave function. Since the population analysis and other one-electron properties are evaluated by expanding the nonatomic part of the wave function about the atoms, the calculation corresponds to a zero-overlap model. Thus, normalization gives the simple result $\alpha' = (1 - \alpha)^{1/2}$ for $7b_{1g}$ and corresponding relations for β' and δ' of the other orbitals in eq 5. The calculated coefficients obtained from the Xα wave function are given in Table VI; Also listed are the crystal field splittings defined in terms of the conventional components $\Delta_\parallel$ and $\Delta_\perp$ (see above).

The ESR spectra are interpreted in terms of the standard spin-Hamiltonian

$$\mathbf{H} = \beta_e \mathbf{H} \cdot \mathbf{g} \cdot \mathbf{S} + \mathbf{I}_{Cu} \cdot \mathbf{A}_{Cu} \cdot \mathbf{S} + \mathbf{I}_N \cdot \mathbf{A}_N \cdot \mathbf{S} \qquad (6)$$

Here H is the external field, **g** is the effective g tensor, β_e is the electronic Bohr magneton, **S** is the electron spin, $\mathbf{I}_{Cu}$ and $\mathbf{I}_N$ are the nuclear spins, and $\mathbf{A}_{Cu}$ and $\mathbf{A}_N$ are nuclear hyperfine tensors; the copper and nitrogen quadrupole couplings are neglected. It is the tensor parameters **g**, $\mathbf{A}_{Cu}$, and $\mathbf{A}_N$ that depend on the wave function of the system.

The g tensor is derived by viewing the d^9 system as a state with a single hole in the $7b_{1g}$ ($3d_{x^2-y^2}$) orbital. Upon application of the spin-orbit perturbation, the pair of first-order wave functions for the lowest Kramers doublet[47] are

$$|+\rangle = \alpha|d_{x^2-y^2}\uparrow\rangle - \frac{i\lambda\beta^2\alpha}{\Delta_\parallel}|d_{xy}\uparrow\rangle + \frac{i\lambda\delta\alpha}{2\Delta_\perp}|d_{yz}\downarrow\rangle - \frac{\lambda\delta^2\alpha}{2\Delta_\perp}|d_{xz}\downarrow\rangle$$

$$|-\rangle = \alpha|d_{x^2-y^2}\downarrow\rangle + \frac{i\lambda\beta^2\alpha}{\Delta_\parallel}|d_{xy}\downarrow\rangle + \frac{i\lambda\delta^2\alpha}{2\Delta_\perp}|d_{yz}\uparrow\rangle + \frac{\lambda\delta^2\alpha}{2\Delta_\perp}|d_{xz}\uparrow\rangle \qquad (7)$$

and the g-tensor values are

$$g_z = g_\parallel = 2.0023 - \frac{8\lambda\alpha^2\beta^2}{\Delta_\parallel}$$

$$g_x = g_y = g_\perp = 2.0023 - \frac{2\lambda\alpha^2\delta^2}{\Delta_\perp} \qquad (8)$$

where λ is the spin-orbit coupling constant for the free ion (-828 cm^{-1} for Cu^{2+}). Ligand contributions to **g**, which are neglected in eq 8, have been shown to be negligible for this system.[43,44]

The magnetic hyperfine Hamiltonian for the interaction of the electron with nucleus N (N = Cu or N)[47] is

$$\mathcal{H}_N = 2\beta_e g_N \beta_N \left\{\frac{\mathbf{I}\cdot\mathbf{I}_N}{r^3} - \frac{\mathbf{S}\cdot\mathbf{I}_N}{r^3} + \frac{3(\mathbf{r}\cdot\mathbf{I}_N)(\mathbf{r}\cdot\mathbf{S})}{r^5}\right\} + 2\beta_e g_N \beta_N \{^8/_3\pi\delta(\mathbf{r})\mathbf{S}\cdot\mathbf{I}_N\} \qquad (9)$$

or

$$\mathcal{H}_N = \mathbf{S}\cdot\mathbf{A}_N\cdot\mathbf{I}_N = \mathbf{S}\cdot\mathbf{A}_N{}^d\cdot\mathbf{I}_N + \mathbf{S}\cdot\mathbf{A}_N{}^c\cdot\mathbf{I}_N \qquad (10)$$

where **r** is the vector from the nucleus to the electron, **S** is the electron spin, I is the orbital angular momentum, and $\mathbf{A}_N{}^d$ and $\mathbf{A}_N{}^c$ are respectively the dipolar and contact contributions to the hyperfine tensor. Taking matrix elements of eq 9 with the Kramers doublet wave functions (eq 7), we obtain the components of the hyperfine tensor for interaction with the copper nucleus. It has the form[47] (again neglecting neighboring atom contributions)

$$A_{zz} = A_\parallel = P\left\{-4/7\alpha^2 - \kappa - 2\lambda\alpha^2\left(\frac{4\beta^2}{\Delta_\parallel} + \frac{3\delta^2}{7\Delta_\perp}\right)\right\}$$

$$A_{xx} = A_{yy} = A_\perp = P\left\{2/7\alpha^2 - \kappa - \frac{11\lambda\alpha^2\delta^2}{7\Delta_\perp}\right\} \qquad (11)$$

In eq 11, κ is introduced (see below) to take account of the Fermi contact contribution and the remaining terms in the expression correspond to the dipolar contribution. The quantity P has the form

$$P = \beta_e g_e \beta_N g_N \langle r^{-3}\rangle_{3d} \qquad (12)$$

where $\langle r^{-3}\rangle_{3d}$ is the value of the radial integral, which in the standard model is assumed to be the same for all of the d orbitals. The free ion value[51] for P for $^{63}Cu^{2+}$ is 0.0388 cm^{-1}. We shall use this value here, pending the fuller discussion given below. MR treated P as an adjustable parameter and assigned a value of 0.0350 cm^{-1} to P for CuTPP containing a natural abundance mixture of ^{65}Cu and ^{63}Cu; the g_N factors for ^{65}Cu and ^{63}Cu are 1.5860 and 1.4804, respectively. In the restricted Hartree-Fock scheme, the spin density at the copper nucleus vanishes, and this is not changed to first order by spin-orbit coupling. Hence, in this simplified picture the value of κ is treated as an adjustable parameter. Its value for a variety of copper compounds has been found to be between 0.30 and 0.35;[49] we use the average value of 0.325 for κ.

With the calculated Xα wave function and the empirical values for λ, κ, and $\langle r^{-3}\rangle_{3d}$, we substitute into the equations to obtain the hyperfine and g-tensor elements shown in Table VII; the experimental estimates of MR are also given. It is evident that the agreement for the quantities $g_\perp$, $g_\parallel$, and $A_\perp{}^d$, $A_\parallel{}^d$ is very good; the agreement for P_κ has no meaning since it is based on fitting the data. The estimates from the extended PPP calculation are also listed in the table and show corresponding agreement. This suggests that both the Xα and PPP electron distributions and state splittings, as well as those estimated by MR from the ESR data, are similar and reasonable. However, it should be mentioned that because the experimental quantities each depend on several of the wave function parameters, values of the former do not give a unique determi-

Table VI. Molecular Orbital Coefficients[a]

	Restricted	Unrestricted
		0.586
α^2	0.617	0.632
		0.906
β^2	0.935	0.943
		0.524
δ^2	0.703	0.765
$\Delta_\parallel$, cm^{-1}	22900	22800
$\Delta_\perp$, cm^{-1}	22800	23100

[a] See text for definitions of symbols; for the unrestricted calculation spin-up values are listed above spin-down.

Table VII. Spin-Restricted ESR Results[a]

	Xα	MR[b]	PPP[c]
$\beta^2/\Delta_\parallel$	4.1×10^{-5} [d]	3.8×10^{-5}	
$\delta^2/\Delta_\perp$	3.1×10^{-5} [d]	3.5×10^{-5}	
α^2	0.62	0.79	0.71
$g_\parallel$	2.170	2.190	2.18
$g_\perp$	2.034	2.045	2.04
P_κ, cm^{-1}	0.0126[e]	0.0126	0.0116
$A_\parallel$, cm^{-1}	−0.0193	−0.0206	−0.0196
$A_\perp$, cm^{-1}	−0.0048	−0.0033	−0.0023

[a] See text for definitions of symbols. [b] From ref 44. [c] From ref 27. [d] With Δ in cm^{-1}. [e] Assumed value, see text.

Table VIII. Superhyperfine Parameters[a]

	Res	Unres	Exptl[b]
a_N	0.00181	0.00173	0.00159
A_N'	0.00167	0.00159	0.00149
B_N'	0.00209	0.00201	0.00179
f_σ/f_s	3.3	3.4	2.1[c]

[a] Values in cm^{-1}. [b] From ref 55. [c] Calculated from eq 13.

nation of the latter; for example, the PPP value of α^2 is 0.712 while that from the restricted Xα calculation is 0.617 (see Table VI). The Xα results are also in agreement with the speculations of MR that there is some out-of-plane π bonding, little or no in-plane π bonding, and $\Delta_\parallel \approx \Delta_\perp \approx 23\,000\ cm^{-1}$. The $6b_{2g}$ orbital has the proper symmetry to form in-plane π bonds, but there is little evidence of this since this orbital has 94% copper $3d_{xy}$ character (see Table VI). On the other hand, the $2e_g$ orbital involves significant contributions from both the copper d_{xz}, d_{yz} and the porphine π orbitals, indicating that there is out-of-plane π bonding.

We consider next the superhyperfine splittings from the ^{14}N nuclei of the porphine ligand. This is again described by the hyperfine Hamiltonian given in eq 9 and 10. Following MR, we assume that the hyperfine tensor is axially symmetric with components $A_\perp = A_N$ and $A_\parallel = B_N$ in the usual notation. The experimental values used in the analysis (A_N', B_N') are corrected for the small direct dipole term, which is estimated by MR to equal $2 \times 10^{-5}\ cm^{-1}$. In the usual theory, A_N' and B_N' are related to the fraction of s and p character on the nitrogen, called f_s and f_σ, respectively, by the equations[47]

$$A_N' = {}^{16}/_{3}\pi\beta_e g_N\beta_N|\phi(2s)|^2 f_s - {}^{4}/_{5}\beta_e g_N\beta_N\langle r^{-3}\rangle_{2p} f_\sigma$$
$$B_N' = {}^{16}/_{3}\pi\beta_e g_N\beta_N|\phi(2s)|^2 f_s + {}^{8}/_{5}\beta_e g_N\beta_N\langle r^{-3}\rangle_{2p} f_\sigma \quad (13)$$

Using the Hartree-Fock-Slater ($\alpha = 1$) values of Hurd and Coodin[52] of 5.6 and 3.6 au respectively for $|\phi(2s)|^2$ and $\langle r^{-3}\rangle_{2p}$ of the nitrogen atom and the hybridization ratio obtained from the Xα wave function, which is shown in Table VIII, we arrive at the values for the superhyperfine tensor given there; a_N is the isotropic hyperfine contribution. The final column lists the experimental values and the hybridization ratio estimated from them with the Hurd and Coodin parameters. Again the agreement with experiment is reasonable, although all of the Xα values are somewhat larger than the experimental results. Use of the more accurate Hartree-Fock values[53] ($|\phi(2s)|^2 = 4.95$ au and $\langle r^{-3}\rangle_{2p} = 3.13$ au) would improve the agreement. The most significant difference is that the calculated (B_N'/A_N') ratio is somewhat too large; this is a direct consequence of the larger (f_σ/f_s) ratio. The excess p_σ character suggests that an sp^2 hybridization does not adequately describe the Xα nitrogen atomic wave function in the $7b_{1g}$ orbital. The experimental fits for both copper tetraphenylporphine[44] and copper phthalocyanine[46] yield a f_σ/f_s ratio considerably closer to 2 (sp^2 hybridization) than the Xα value. However, some care must be used in interpreting the Xα results because of the finite radii of the atomic orbitals and the resulting difference in the expectation values obtained from them (see below). Also, it may be noted that the EHT calculation gives a large amount of nitrogen p character to the $7b_{1g}$ antibonding orbital. Comparison with the PPP calculation for the isotropic term a_N shows similar agreement to that obtained from the Xα wave function, while a CNDO calculation[54] gave less than half of the observed splitting; neither of those papers gave the individual A_N', B_N' values.

Very recently,[55] ENDOR measurements on CuTPP have been used to determine the hyperfine tensor for protons at the C_β position. The experimental principal components are 8.4, 2.4, and $2.7 \times 10^{-5}\ cm^{-1}$. The calculated tensor arises from the spin distribution in the $7b_{1g}$ orbital;[56] we obtain the values 8.1, 1.3, and $0.7 \times 10^{-5}\ cm^{-1}$. Important contributions to the anisotropic part come from the copper (~50%), from the nearest N (~25%), and from the neighboring C_β (20%). The isotropic Fermi contact contribution, which is one-third the trace of this tensor, is $4.4 \times 10^{-5}\ cm^{-1}$ in the experiment and $3.4 \times 10^{-5}\ cm^{-1}$ in the calculation. The calculation corresponds to a spin density of $2.5 \times 10^{-4} a_0^{-3}$ or a spin population in the hydrogen 1s orbital of 7.1×10^{-4} electron. This is the result of σ spin transfer through four bonds, so that the agreement with experiment is encouraging.

(IV) Extended Treatment

In this section we consider three effects that appear in a more complete calculation of the ESR parameters; depending on their importance, these effects can alter the conventional interpretation of ESR experiments. First, an unrestricted wave function is used so that the unpaired electron in the $7b_{1g}$ orbital can induce a net spin polarization in the other occupied orbitals; second, excited states in addition to those included in the simple picture are allowed to mix with the ground state by spin-orbit coupling; and finally, the radial behavior of the copper 3d orbitals is calculated for the molecule instead of being taken from the free ion. None of the resulting refinements produce changes that are large enough to invalidate the interpretation of the ESR spectrum given above for the copper pophyrins, but each is significant and must be considered if careful quantitative comparisons between theory and experiment are to be made.

Spin Polarization. One-electron energies and populations from the spin unrestricted Xα method[5] have already been used (section III; Tables II, III, and V). For electronic transitions or redox behavior the use of unrestricted energies gives slightly different numerical results from the restricted calculation but the qualitative interpretation is the same. This is not the case for the ESR parameters; the most obvious effect is on the isotropic hyperfine splitting due to the copper nuclear spin, which vanishes in a restricted wave function. Here we describe this and other aspects of the ESR analysis which are significantly affected by the use of a spin unrestricted wave function.

The coefficients of the molecular orbitals most important for the ESR analysis (see eq 5) are given in Table VI. Both restricted and unrestricted values are given; for the latter, the number of spin-up electrons is taken to be greater than the number of spin-down electrons. The copper "character" of the unrestricted 3d-like molecular orbitals brackets the restricted values. The difference between spin-up and spin-down is most pronounced in the $d\pi$ orbitals (involving δ^2) where it is nearly 25%. These coefficients are important for the interpretation of ESR results since they determine the magnitude of the spin-orbit contribution to the g and hyperfine tensors.

Evaluation of the g tensor is complicated by the fact that the unrestricted wave function is not a spin eigenfunction. In particular, the perpendicular component of $\mathbf{g}$ can deviate from the free-electron value even in the absence of spin-orbit coupling. To demonstrate this, we consider a model three-electron problem with a wave function of the form

$$|0\alpha\rangle = |\phi_1\bar{\phi}_1'\phi_2| \quad (14a)$$

where ϕ_1, ϕ_1' are the two different spatial parts of orbital 1, with ϕ_1 (ϕ_1') that of majority (minority) spin; ϕ_2 is orthogonal to both ϕ_1 and ϕ_1' and $\langle\phi_1|\phi_1'\rangle = \Delta_1$. For the copper porphine system the function ϕ_2 would represent the spatial part of the unpaired ($7b_{1g}$) orbital, while ϕ_1 and ϕ_1' would correspond to the spatial parts of orbitals of b_{2g} or e_g symmetry that would be identical in a restricted calculation. A bar indicates a spin-down orbital, and unbarred orbitals are spin-up. Thus $|0\alpha\rangle$ is an eigenfunction of S_z with $M_s = 1/2$. The corresponding

function with $M_s = -1/2$ is obtained by interchanging the spin-up and spin-down orbitals; that is,

$$|0\beta\rangle = |\overline{\phi_1}\phi_1'\overline{\phi_2}| \tag{14b}$$

If we now evaluate matrix elements of the Zeeman operator $g_e\beta_e\mathbf{S}\cdot\mathbf{H}$ with eq 14, there are diagonal elements with the field parallel to $\hat{\mathbf{z}}$ and off-diagonal elements with the field perpendicular to $\hat{\mathbf{z}}$. The former yield $g_\parallel = g_e$, while the latter give $g_\perp = g_e\Delta_1^2$, with $\Delta_1 \leq 1$. This deviation from the spin-only value is a consequence of the properties of the unrestricted wave function. If a spin eigenfunction with $S = 1/2$ is constructed from it by projection,

$$|0\alpha\rangle^P = \omega^{-1/2}\{(2/3)|0\alpha\rangle - (1/3)|\phi_1\phi_1'\overline{\phi_2}| - (1/3)|\overline{\phi_1}\phi_1'\phi_2|\} \tag{15}$$

with the normalization constant, ω, equal to

$$\omega = 2/3 + 1/3\Delta_1^2 \tag{16}$$

the spin-only value is recovered.

We now consider the effects of spin-orbit coupling, which mixes into the ground state (as given by eq 15) excited configurations of the form

$$|1\alpha\rangle = |\phi_2\overline{\phi}_2\phi_1|, |1\beta\rangle = |\phi_2\overline{\phi}_2\overline{\phi}_1| \tag{17}$$

For simplicity we assume that the $\phi_2(b_{1g})$ orbital is unaffected by spin polarization, so that these determinants are already spin eigenfunctions. To a first approximation, the orbital ϕ_1' does not appear in eq 17 since in each case the orbital of that symmetry is of majority spin, which by definition is ϕ_1. If we apply second-order perturbation theory including both the Zeeman and spin-orbit terms,[57] we obtain the g tensor with elements

$$g_{\alpha\alpha} = g_e + 2|\lambda|\frac{\langle\phi_2|l_\alpha|\phi_1\rangle \cdot \langle\phi_1'|l_\alpha|\phi_2\rangle}{E_1 - E_0}Q\omega^{-1} \tag{18}$$

where

$$Q = 2/3\Delta_1 + 1/3\{\langle\phi_2|l_\alpha|\phi_1'\rangle/\langle\phi_2|l_\alpha|\phi_1\rangle\} \tag{19}$$

and $E_1 - E_0 = \Delta_\parallel(\Delta_\perp)$ if ϕ_1 and ϕ_1' are of $b_{2g}(e_g)$ symmetry. This expression is similar in form to the standard restricted result in eq 8. Aside from the "correction factor" Q/ω, it is the average character of the spin-up and spin-down orbitals that determines the deviations of the g tensor from g_e. This justifies in part the use of a spin-restricted theory, for which the orbitals are intermediate between the corresponding unrestricted ones (see Table VI). The orbital overlap Δ_1 enters both Q and ω, and the ratio (Q/ω) depends upon the magnitudes of Δ_1 and the orbital reduction factors $\langle\phi_2|l_\alpha|\phi_1\rangle$ and $\langle\phi_2|l_\alpha|\phi_1'\rangle$. The orbital overlaps can be evaluated under the approximations used for one-electron properties.[11] The only pair of orbitals for which Δ_1 is significantly less than unity is $2e_g$, for which $\Delta_1 = 0.953$, and hence $\omega = 0.969$. If we assume that $\langle 7b_{1g}|l_\perp|2e_g\downarrow\rangle/\langle 7b_{1g}|l_\perp|2e_g\uparrow\rangle \simeq \delta\downarrow/\delta\uparrow = 1.208$ (cf. Table VI) the correction factor $Q/\omega \simeq 1.071$. (These corrections have a more complicated form if more than three electrons are involved.) With this result we can compare the restricted and unrestricted contributions of the $2e_g$ orbital to the g tensor:

$$\Delta g_\perp(\text{restricted}) = \frac{2|\lambda|\alpha^2\delta^2}{\Delta_\perp} = 0.0315$$

$$\Delta g_\perp(\text{unrestricted}) = \frac{2|\lambda|\alpha^2(\delta\uparrow)(\delta\downarrow)Q}{\Delta_\perp\omega} = 0.0304$$

For this case the two values are nearly identical.

Although spin projection is a well-defined procedure, perturbation theory indicates that it does not result in an improved description of the magnetic properties of molecules.[58] We hope to study this problem in more detail in the future, particularly for systems where $S \geq 1$ and spin polarization effects become increasingly important. The detailed application of eq 18 is postponed until that time.

Table IX. Spin-Unrestricted ESR Parameters[a]

	Xα	MR[b]
a_{Cu}[c]		
1s	−0.0004	
2s	−0.016	
3s	+0.011	
4s	−0.002	
Net	−0.0084	−0.0125
$A^d_\parallel$, cm^{-1} [d]	−0.0160	−0.0158
$A^d_\perp$, cm^{-1}	0.0080	0.0079
$A_\parallel^{so}$ [e]	0.0070	0.0076
$A_\perp^{so}$	0.0010	0.0012
$A_\parallel$[f]	−0.0174	
$A_\perp$	0.0006	
$A_\parallel$[g]	−0.0215	−0.0206
$A_\perp$	−0.0035	−0.0033

[a] All values in cm^{-1}. [b] From ref 44. [c] Fermi contact coupling. [d] First term of eq 11. [e] Last term of eq 11. [f] Sum of contact, direct dipolar, and spin-orbit terms. [g] Assuming $a_{Cu} = -0.0125$, see text.

For the hyperfine tensor we follow eq 11. There are three contributions: the Fermi contact term, the direct dipolar term, and the indirect dipolar term arising from excited configurations that mix with the ground state by spin-orbit coupling.

For the contact term, which was an adjustable parameter in the spin restricted calculation, we now investigate how the unpaired electron induces a net spin density at the copper nucleus. The results are given in Table IX. The largest contributions are from the 2s and 3s orbitals. Both the 2s and 3s spin-up orbital energies are lower than their spin-down counterparts, but the difference in nodal structure leads to densities at the nucleus of opposite sign. This behavior is similar to that seen in ab initio unrestricted Hartree-Fock calculations on the first-row transition elements.[59] Both the 1s and "4s" contributions (the net from all the valence a_{1g} orbitals) are small and negative. Unfortunately, no direct experimental determination of the contact term can be made for transition metal complexes, unlike organic radicals for which the hyperfine behavior can be decomposed to good approximation into contact and dipolar terms. This is because the spin-orbit term, which makes a significant contribution to the hyperfine tensor, is neither isotropic nor traceless. The calculated value can be compared, however, with the results deduced by MR in their analysis of the ESR spectrum based on the spin-restricted theory; their value is -0.0126 cm^{-1}, about 50% larger than the Xα result. Similar deviations were found in an Xα calculation on the Mn^{2+} ion,[60] which gave a smaller spin density at the nucleus than did an unrestricted Hartree-Fock (UHF) calculation; the contribution from each of the inner shells was 30–65% larger in the Hartree-Fock calculation. For neutral atoms of the first transition series, the UHF result gives about 3/4 of the observed spin densities.[61] Nothing definite is known about the corresponding errors in ions bound to ligands, but if they are similar we may expect to find the Xα Fermi contact shifts to be consistently too small.

The direct dipolar coupling term can be calculated from the wave function by means of the one-electron expectation value procedure.[11] It is almost entirely due to the unpaired electron in the $7b_{1g}\uparrow$ orbital, which yields $A_\parallel^d = -0.0162$ cm^{-1}, $A_\perp^d = -1/2A_\parallel^d$. The contribution from all other orbitals, resulting from slight differences in spin-up and spin-down orbitals, is

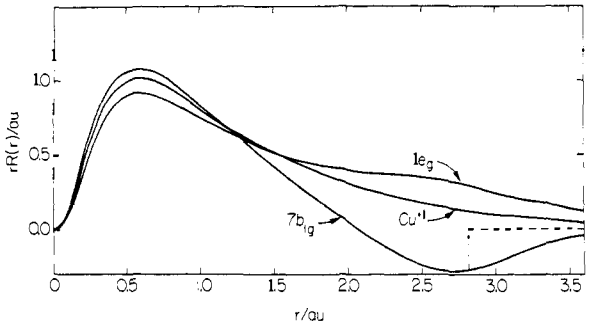

Figure 3. Radial portion of copper 3d orbitals, from the restricted calculation and from a restricted atomic calculation for Cu^+ ($3d^9 4s$). The portion of the $7b_{1g}$ curve under the dashed line is outside the expanded sphere radius.

0.0002 cm^{-1}. This result may be compared to $A_\parallel^d = -0.0158$ cm^{-1}, estimated by MR from the spectral fit. Despite the close agreement between the two values, the orbital descriptions are different. To good approximation the direct contribution to $A_\parallel^d$ is $-\frac{4}{7}g_c\beta_c g_N\beta_N\alpha^2\langle r^{-3}\rangle_{3d}$ (cf. eq 11) since our calculations show that the ligand contribution is less than 1% of the total. MR used $\langle r^{-3}\rangle_{3d} = 7.5a_0^{-3}$, which was an adjustable parameter, and $\alpha^2 = 0.789$, based on an analysis of the superhyperfine splittings. The Xα calculation gives $\alpha^2 = 0.617$ (Table VI) and $\langle r^{-3}\rangle_{3d} = 9.6a_0^{-3}$ for the $7b_{1g}$ orbital (see below).

If we assume the spin-orbit contribution to be the same as that obtained in the restricted calculation, we can add together the Fermi contact, direct dipolar, and spin-orbit terms to obtain a new Xα estimate of the complete hyperfine tensor. The result, given in Table IX, is in poor agreement with the experimental value; it even has the wrong sign for $A_\perp$. Most of the error comes from the contact term calculation. If we assume, as was the case for Mn^{2+}, that the Xα inner shell polarization is only two-thirds of its actual value, we achieve essentially exact agreement with experiment (see Table IX). We conclude that the polarization of inner shells is insufficiently accurate to allow the Xα theory to be used in a completely a priori way but that other parameters obtained from an Xα calculation give satisfactory agreement with experiment. Further, it is clear that occupation coefficients that differ from those estimated by MR can give satisfactory results.

Finally, we consider the superhyperfine splitting involving the porphyrin nitrogens. This is dominated by the Fermi contact term, and the effect of spin polarization is to reduce the coupling constant from that found in the restricted calculation. The uncorrected result from the unrestricted wave function is given in Table VIII. If we assume that the inner shell polarization is again underestimated, the calculated value would be even closer to the experimental coupling. In any case, the agreement is satisfactory considering the sensitivity of this parameter to the amount of copper-ligand mixing.

As with the g tensor, there is an uncertainty about the effects of spin contamination on the magnetic hyperfine parameters. Spin projection is often used to approach this question, although it is not clear that this will lead to improved spin densities.[58] We can consider the effects of projection by returning to the three-electron example, which has the projected density

$$\rho^z(\mathbf{r}_0) \equiv {}^P\langle 0\alpha|\delta(\mathbf{r}-\mathbf{r}_0)2S_z|0\alpha\rangle^P$$
$$= \omega^{-1}\{\tfrac{4}{9}\phi_1^2(\mathbf{r}_0) + \tfrac{1}{9}(4+5\Delta_1^2)\phi_2^2(\mathbf{r}_0) - \tfrac{2}{9}\phi_1'^2(\mathbf{r}_0) - \tfrac{2}{9}\phi_1(\mathbf{r}_0)\phi_1'(\mathbf{r}_0)\Delta_1\} \quad (20)$$

For the copper porphyrin Fermi contact term, we would take ϕ_1 and ϕ_1' to be core s orbitals and $\mathbf{r}_0$ to be the position of the copper nucleus; then $\phi_2(\mathbf{r}_0) = 0$ since it is a d orbital. The unprojected density is simply $\phi_1^2(\mathbf{r}_0) - \phi_1'^2(\mathbf{r}_0)$. In the limit that $\Delta_1 \simeq 1$, the ratio of the projected to unprojected spin densities is $\frac{1}{3}$; this may be derived by writing $\phi_1(\mathbf{r}_0) = \phi_1'(\mathbf{r}_0) + \delta$ and expanding eq 20 to first order in δ. The same ratio is also found for systems with more than three electrons.[62] Hence spin projection, if used, would reduce the calculated contact term and increase the disagreement with experiment.

Table X. Additional Molecular Orbital Coefficients

Orbital	Fraction Cu d orbital[a]	Δ, cm^{-1} [b]	Δg[c]
$5b_{2g}$	0.047	50,700	0.0038
$1e_g$	0.275	42,300	0.0066
$4e_g$	0.041	9,900	0.0042

[a] For the b_{2g} orbital, this is the analogue of β^2; for the e_g orbitals, it is the analogue of δ^2. [b] For the b_{2g} orbital this is the analogue of $\Delta_\parallel$; for the e_g orbitals it is the analogue of $\Delta_\perp$ (From Table V). [c] Contribution to g tensor, from eq 8.

Additional Excited Configurations. Table X gives the fractional copper contribution and excitation energy for three additional orbitals which have significant copper occupation and which have the proper symmetry to contribute by spin-orbit coupling to the g tensor and hyperfine splittings. The energies were estimated from the transition-state calculation described earlier (see Table V). These orbitals contribute to the g tensor in accord with their symmetries; i.e., the b_{2g} contributes to $g_\parallel$ and the e_g to $g_\perp$. In the spin-restricted theory the contributions of these orbitals can be obtained from eq 8; values are shown in Table X. Adding the two e_g orbital contributions to the one shown in Table VI we find an effective value of "$\delta^2/\Delta_\perp$" of 4.2×10^{-5}, with $\Delta_\perp$ expressed in cm^{-1}. This "extra" π orbital contribution amounts to ~25% of the total shift of $g_\perp$ from the spin-only value and emphasizes that fits to experimental data determine only effective parameters rather than the coefficients of particular orbitals. Thus, too great a reliance on the simple ligand field theory may lead to misinterpretation of the nature of the metal-ligand bonding. We expect this to be true for other organometallic complexes where the ligand π orbitals have the proper energy to mix with the dπ orbitals of the metal.

Copper 3d Radial Functions. The radial behavior of the copper 3d orbitals is not fixed in an Xα calculation, so that the parameters P and λ, both of which depend upon $\langle r^{-3}\rangle_{3d}$, vary from one orbital to another and deviate from the free ion values. In an empirical analysis, such as that of MR, these deviations are neglected. In Table XI we give some information about the radial dependence of molecular orbitals having significant copper 3d character. Values of $\langle r^{-3}\rangle$ are obtained from

$$\langle r^{-3}\rangle = \int_0^{b_\alpha} r^{-3}(R(r))^2 r^2\,dr \Big/ \int_0^{b_\alpha} (R(r))^2 r^2\,dr \quad (21)$$

where $R(r)$ is the radial function for the particular 3d orbital and b_α is the expanded sphere radius[11] for copper; the expectation value is normalized to unit charge in the 3d orbital. For Cu^{2+}, the Xα value of $\langle r^{-3}\rangle$ is ~3% larger than the corresponding Hartree-Fock value.[59] For the copper orbitals as part of the molecular orbitals in CuP Table XI shows that there is a significant variation. Orbitals with higher energies generally have larger values of $\langle r^{-3}\rangle$, and therefore of P, than the lower lying orbitals. Similar behavior has been seen in extended basis ab initio calculations of transition metal complexes.[63] This behavior is illustrated in Figure 3, where the strongly antibonding $7b_{1g}$ orbital is seen to have a node near $r = 2a_0$, while the bonding $1e_g$ orbital has no node. The relative contraction

Table XI. Radial Behavior of Copper d Orbitals[a]

	Energy, eV	% 3d	Δq^b	$\langle r^{-3}\rangle$, au	λ', cm^{-1}	P, cm^{-1} [c]
Atom:[d]						
Cu^0	−9.54	100.0	1.7	8.30	−974	0.0391
Cu^+	−18.81	100.0	1.2	8.37	−981	0.0394
Cu^{2+}	−29.48	100.0	1.0	8.47	−993	0.0399
Molecule:						
$4b_{1g}\uparrow$	−17.31	14.6	8.7	3.85	−441	0.0181
$\downarrow$	−17.21	11.9	10.2	3.36	−384	0.0158
$6b_{1g}\uparrow$	−14.21	26.9	1.5	6.63	−771	0.0312
$\downarrow$	−14.00	30.0	1.9	6.02	−699	0.0283
$7b_{1g}\uparrow$	−9.31	58.6	1.6	9.57	−1128	0.0451
$\downarrow$	−8.69	63.2	1.4	9.50	−1119	0.0448
$5b_{2g}\uparrow$	−13.75	7.4	3.1	6.92	−806	0.0326
$\downarrow$	−13.69	3.9	5.0	6.09	−708	0.0287
$6b_{2g}\uparrow$	−12.26	90.6	0.4	8.36	−979	0.0394
$\downarrow$	−11.52	94.3	0.6	8.20	−959	0.0386
$1e_g\uparrow$	−13.07	46.2	4.9	7.35	−859	0.0346
$\downarrow$	−12.80	20.4	8.2	6.60	−769	0.0311
$2e_g\uparrow$	−12.09	52.4	0.9	8.44	−989	0.0398
$\downarrow$	−11.56	76.5	1.7	8.08	−944	0.0381

[a] Values are normalized to unit charge in the 3d orbital. [b] Percent of column 3 that lies outside $r = 2.62a_0$. [c] For ^{63}Cu, from eq 12. [d] Configurations are $3d^9$, $3d^94s$, and $3d^94s^2$, respectively.

of the antibonding orbitals places more charge near the copper nucleus and increases the value of $\langle r^{-3}\rangle$, a trend well known in model studies.[64] The variations shown in Table XI are similar in magnitude and direction to those calculated by Belford and Karplus[64] with a point charge model for the ligands. An expanded version of eq 11 which takes cognizance of this variation has the form

$$A_\parallel^{\,d} = -\tfrac{4}{7}\alpha^2 P(b_{1g}) - \frac{8\lambda\alpha^2\beta^2 P(b_{2g})}{\Delta_\parallel} - \frac{6\lambda\alpha^2\delta^2 P(e_g)}{7\Delta_\perp}$$

$$A_\perp^{\,d} = \tfrac{2}{7}\alpha^2 P(b_{1g}) - \frac{11\lambda\alpha^2\delta^2 P(e_g)}{7\Delta_\perp} \qquad (22)$$

where

$$P(\phi) = g_e\beta_e g_N\beta_N\langle 7b_{1g}|r^{-3}|\phi\rangle \qquad (23)$$

The orbitals in eq 5 make the most important contribution to A^d. Since these have similar values of $\langle r^{-3}\rangle$, we can make a rough estimate of $P(\phi)$ from the diagonal expectation values given in Table XI: $P(7b_{1g}) = 0.045$ cm^{-1}, $P(6b_{2g}) \simeq P(2e_g) \simeq 0.041$ cm^{-1}. The former value is significantly larger than the value of 0.0388 cm^{-1} assumed by MR.

A corresponding question exists concerning the values for λ. In Table XI we give a calculation of λ', obtained from the formula

$$\lambda' = \frac{-\hbar^2}{2m^2c^2}\left\langle \frac{1}{r}\frac{dV}{dr}\right\rangle_{3d} \equiv -\frac{e^2\hbar^2 Z'}{2m^2c^2}\langle r^{-3}\rangle_{3d} \qquad (24)$$

where Z' is defined by the last equation and varies from 19.6 to 20.2 for these orbitals. The minus sign arises because we treat the states as single holes in a closed 3d shell. Blume and Watson[65] have shown that eq 24 does not correctly include the exchange contributions, which shield the nucleus to a significant extent. For Cu^{2+}, λ' as calculated from eq 24 is ~20% above the Blume and Watson value including exchange, which is identical with the empirical value of −828 cm^{-1} used by MR. Therefore, the values given in Table XI probably overestimate the spin-orbit coupling by a corresponding amount. Nevertheless, they show clearly the variation to be expected among the different orbitals. The parameter λ of eq 7 is an off-diagonal element, $\langle 3d_{xy}|\mathcal{H}_{so}|3d_{x^2-y^2}\rangle$ or $\langle 3d\pi|\mathcal{H}_{so}|3d_{x^2-y^2}\rangle$, and should fall between the corresponding diagonal elements shown in the table. Based on these considerations, we expect λ to be nearly the same for the $6b_{2g}$ (d_{xy}) and $2e_g$ ($d\pi$) orbitals and to be 5-10% larger than the value for free Cu^{2+}.

The effects of radial variation can be estimated by recalculating the hyperfine tensor in the restricted theory using eq 11, with $\lambda = -900$ cm^{-1}, $P_K = 0.0126$ cm^{-1}, and the P values for $7b_{1g}$, $6b_{2g}$, $2e_g$ given above. The result is $A_\parallel = -0.0203$ cm^{-1} and $A_\perp = -0.0034$ cm^{-1}, in excellent agreement with the experimental values. The improvement over the results in Table VII comes mainly from the increased value of $\langle r^{-3}\rangle_{3d}$ for the $7b_{1g}$ orbital, as we discussed above. The radial compression of strongly antibonding orbitals should be kept in mind when assigning orbital coefficients from ESR data.

Conclusion

In this paper we have applied the Xα method to copper porphine and demonstrated that valid results are obtained for its electronic structure and spectra. This is the first time that the Xα method has been employed for such a large organometallic system. The interpretation of the electronic structure of organometallic complexes is such a difficult task that it is useful to have a number of theoretical approaches that can be applied to specific problems. For some properties, the Xα method yields interpretations that differ from previously applied methods. Comparison with experiment for the oxidation-reduction behavior indicates that the present results are more satisfactory; for other features, such as the electronically excited states, the experimental evidence is ambiguous. Excellent agreement is obtained with the observed ESR spectrum. The present calculation emphasizes the importance of radial variation in the copper 3d orbitals and of additional orbitals which are ignored in ligand-field calculations. Additional studies are needed on organometallic complexes to confirm the reliability of the method. However, even from the present calculation it is clear that the Xα multiple scattering method should become an increasingly important tool for the understanding of the properties of such systems.

Acknowledgments. We thank Keith Johnson for the Xα program and for helpful comments on the work. Most of the calculations were done at the CIRCE, Orsay, France.

References and Notes

(1) (a) Supported by a grant from the National Science Foundation (CHE 76-17569) and the Centre National de la Recherche Scientifique; (b) National Science Foundation Predoctoral Fellow (1970–1974).
(2) (a) J. E. Falk, "Porphyrins and Metalloporphyrins", Elsevier, Amsterdam, 1964; (b) P. W. Lau and W. C. Lin, *J. Inorg. Nucl. Chem.*, **37**, 2389 (1975), and references therein.
(3) W. S. Caughey, R. M. Deal, C. Weiss, and M. Gouterman, *J. Mol. Spectrosc.*, **16**, 415 (1965).
(4) Y. Niwa, *J. Chem. Phys.*, **62**, 737 (1975).
(5) J. C. Slater, "Quantum Theory of Molecules and Solids", Vol IV, McGraw-Hill, New York, N.Y., 1974.
(6) K. H. Johnson, *Annu. Rev. Phys. Chem.*, **26**, 39 (1975); *Adv. Quantum Chem.*, **7**, 143 (1973).
(7) J. W. D. Connolly, "Modern Theoretical Chemistry", Vol. IV, G. A. Segal, Ed., Plenum Press, New York, N.Y., 1976.
(8) N. Rosch and K. H. Johnson, *Chem. Phys. Lett.*, **24**, 179 (1974).
(9) N. Rosch, R. P. Messmer, and K. H. Johnson, *J. Am. Chem. Soc.*, **96**, 3855 (1974).
(10) A. R. Williams, *Int. J. Quantum Chem., Symp.*, **8**, 89 (1974).
(11) D. A. Case and M. Karplus, *Chem. Phys. Lett.*, **39**, 33 (1976).
(12) N. H. F. Beebe, *Chem. Phys. Lett.*, **19**, 290 (1973).
(13) O. Goscinski, B. T. Pickup, and G. Purvis, *Chem. Phys. Lett.*, **22**, 167 (1973).
(14) L. J. Radonovitch, A. Bloom, and J. L. Hoard, *J. Am. Chem. Soc.*, **94**, 2073 (1972).
(15) J. L. Hoard, *Science*, **134**, 1295 (1971).
(16) E. B. Fleischer, C. K. Miller, and L. E. Webb, *J. Am. Chem. Soc.*, **86**, 2342 (1964).
(17) K. Schwarz, *Phys. Rev. B*, **5**, 2466 (1972); K. Schwarz and J. W. D. Connolly, *J. Chem. Phys.*, **55**, 4710 (1971).
(18) J. C. Slater, *Int. J. Quantum Chem., Symp.*, **7**, 533 (1973).
(19) N. Rosch, W. G. Klemperer, and K. H. Johnson, *Chem. Phys. Lett.*, **23**, 149 (1973).
(20) F. Herman, A. R. Williams, and K. H. Johnson, *J. Chem. Phys.*, **61**, 3508 (1974).
(21) F. Herman, W. E. Rudge, I. P. Batra, and B. I. Bennett, *Int. J. Quantum Chem., Symp.*, **10**, 167 (1976), and references therein.
(22) I. P. Batra and O. Robaux, *Chem. Phys. Lett.*, **28**, 529 (1974).
(23) J. G. Norman, Jr., *J. Chem. Phys.*, **61**, 4630 (1974); *Mol. Phys.*, **31**, 1191 (1976).
(24) D. A. Case and M. Karplus, to be published; D. A. Case, Ph.D. Thesis, Harvard University, 1977.
(25) J. G. Norman, Jr., and S. C. Jackels, *J. Am. Chem. Soc.*, **97**, 3822 (1975); see also J. G. Norman, Jr., *Mol. Phys.*, **31**, 1191 (1976).
(26) M. Zerner and M. Gouterman, *Theor. Chim. Acta*, **4**, 44 (1966).
(27) B. Roos and M. Sundbom, *J. Mol. Spectrosc.*, **36**, 8 (1970).
(28) M. Zerner, M. Gouterman, and H. Kobayashi, *Theor. Chim. Acta*, **6**, 363 (1966).
(29) D. W. Turner, C. Baker, A. D. Baker, and C. R. Brundle, "Molecular Photoelectron Spectroscopy", Wiley, New York, N.Y., 1970; see also D. H. Karweik and N. Winograd, *Inorg. Chem.*, **15**, 2336 (1976), and references therein.
(30) J. Demuynck and A. Veillard, *Chem. Phys. Lett.*, **6**, 204 (1970).
(31) A. Stanienda, *Z. Naturforsch., B*, **23**, 1285 (1968).
(32) S. C. Kandeiwal and J. L. Roebber, *Chem. Phys. Lett.*, **34**, 355 (1975).
(33) S. Cradock, R. H. Findlay, and M. H. Palmer, *Tetrehedron*, **29**, 2173 (1973).
(34) See, e.g., L. Salem, "The Molecular Orbital Theory of Conjugated Systems", W. A. Benjamin, New York, N.Y., 1966, pp 152–158.
(35) D. Dolphin and R. H. Felton, *Acc. Chem. Res.*, **7**, 26 (1974), and references therein.
(36) R. H. Felton and H. Linschitz, *J. Am. Chem. Soc.*, **88**, 1113 (1966).
(37) C. Weiss, H. Kobayashi, and M. Gouterman, *J. Mol. Spectrosc.*, **16**, 445 (1965).
(38) D. W. Thomas and E. E. Martell, *Arch. Biochem. Biophys.*, **76**, 286 (1958).
(39) R. L. Ake and M. Gouterman, *Theor. Chim. Acta*, **15**, 20 (1969); D. Eastwood and M. Gouterman, *J. Mol. Spectrosc.*, **30**, 437 (1969).
(40) M. Gouterman, L. K. Hanson, G. E. Riehl, W. R. Lehnstra, and J. W. Buchler, *J. Chem. Phys.*, **62**, 2343 (1975).
(41) C. M. Guzy, J. B. Raynor, and M. C. R. Symons, *J. Chem. Soc. A*, 2299 (1969).
(42) E. M. Roberts and W. S. Koski, *J. Am. Chem. Soc.*, **82**, 3006 (1960).
(43) J. M. Assour, *J. Chem. Phys.*, **43**, 2477 (1965). The value of $g_\perp$ from this study is not in agreement with other experiments.
(44) P. T. Manoharan and M. T. Rogers, "Electron Spin Resonance of Metal Complexes", T. F. Yeh, Ed., Adam Hilger, New York, N.Y., 1969, p 143.
(45) S. E. Harrison and J. M. Assour, *J. Chem. Phys.*, **40**, 365 (1964).
(46) C. M. Guzy, J. B. Raynor, L. P. Stodulski, and M. C. R. Symons, *J. Chem. Soc. A*, 997 (1969).
(47) H. A. Kuska and M. T. Rogers, "Spectroscopy in Inorganic Chemistry", Vol. 2, Academic Press, New York, N.Y., 1971, p 175. See also A. Abragam and B. Bleany, "Electron Paramagnetic Resonance of Transition Ions", Clarendon, New York, N.Y., 1970.
(48) A. Abragam and M. H. L. Pryce, *Proc. R. Soc. London, Ser. A*, **205**, 135 (1951); 206, 164 (1951).
(49) A. H. Maki and B. R. McGarvey, *J. Chem. Phys.*, **29**, 31, 35 (1958).
(50) D. Kivelson and R. Nieman, *J. Chem. Phys.*, **35**, 149 (1961).
(51) B. R. McGarvey, *J. Phys. Chem.*, **71**, 51 (1967).
(52) C. M. Hurd and P. G. Coodin, *J. Phys. Chem. Solids*, **28**, 523 (1966).
(53) D. R. Hartree and W. Hartree, *Proc. R. Soc. London, Ser. A*, **193**, 299 (1948); see also ref 49.
(54) D. W. Clack and M. S. Farrimond, *J. Chem. Soc., Dalton Trans.*, 29 (1972).
(55) T. G. Brown, J. L. Petersen, G. P. Lozos, J. R. Anderson, and B. M. Hoffman, *Inorg. Chem.*, **16**, 1563 (1977).
(56) H. M. McConnell and J. Strathdee, *Mol. Phys.*, **2**, 129 (1959).
(57) C. P. Slichter, "Principles of Magnetic Resonance", Harper and Row, New York, N.Y., 1963.
(58) P. J. Rossky and M. Karplus, to be published.
(59) R. E. Watson and A. J. Freeman, *Phys. Rev.*, **123**, 2027 (1961).
(60) T. M. Wilson, J. H. Wood, and J. C. Slater, *Phys. Rev. A*, **2**, 620 (1970); see also P. E. Desmier, M. A. Whitehead, R. Bogdanovoć, and M. S. Gopinathan, *Mol. Phys.*, **33**, 1457 (1977).
(61) P. S. Bagus, B. Liu, and H. F. Schaefer III, *Phys. Rev. A*, **2**, 555 (1970).
(62) J. E. Harriman, "La Structure Hyperfine Magnétique des Atomes et des Molécules", Editions du Centre National de la Recherche Scientifique, Paris, 1967, p 139.
(63) See, e.g., J. W. Moscovitz, C. Hollister, C. J. Hornback, and M. Basch, *J. Chem. Phys.*, **53**, 2570 (1970); H. M. Gladney and A. Veillard, *Phys. Rev.*, **180**, 385 (1969).
(64) R. L. Belford and M. Karplus, *J. Chem. Phys.*, **51**, 394 (1959); W. Marshall and R. Stuart, *Phys. Rev.*, **123**, 2048 (1961).
(65) M. Blume and R. E. Watson, *Proc. R. Soc. London, Ser. A*, **270**, 127 (1962); **271**, 565 (1963).